Title: Light Activated BioID (LAB): an optically activated proximity labeling system to study protein-protein interactions.

Authors: Omer Shafraz [‡], Carolyn Marie Orduno Davis [‡], Sanjeevi Sivasankar [*].

Affiliation: Department of Biomedical Engineering, University of California, Davis, 95616, CA.

[‡] Contributed equally to this work.

* To whom correspondence should be addressed. Email: ssivasankar@ucdavis.edu.

Abstract

Proximity labeling with genetically encoded enzymes is widely used to study protein-protein interactions in cells. However, the resolution and accuracy of proximity labeling methods are limited by a lack of control over the enzymatic labeling process. Here, we present a high spatial and temporal resolution technology that can be activated on demand using light, for high accuracy proximity labeling. Our system, called Light Activated BioID (LAB), is generated by fusing the two halves of the split-TurboID proximity labeling enzyme to the photodimeric proteins CRY2 and CIB1. Using live cell imaging, immunofluorescence, western blotting, and mass spectrometry, we show that upon exposure to blue light, CRY2 and CIB1 dimerize, reconstitute the split-TurboID enzyme, and biotinylate proximate proteins. Turning off the light halts the biotinylation reaction. We validate LAB in different cell types and demonstrate that it can identify known binding partners of proteins while reducing background labeling and false positives.

Introduction:

Protein-protein interactions (PPIs) are essential for cellular function and decoding these interactions are crucial to understanding biological pathways in health and disease. While many methods have been developed to map protein interactomes (Qin et al. 2021), proximity labeling (PL) techniques are among the most widely used approaches, since they capture transient, dynamic PPIs in the near-native cellular environment.

PL employs enzymes such as promiscuous biotin ligases for proximity-dependent biotin identification (BioID) (Choi-Rhee et al. 2004, Roux et al. 2012, Kim et al. 2016, Ramanathan et al. 2018), peroxidases for peroxide-dependent biotin identification (APEX) (Martell et al. 2012), horseradish peroxidase (HRP) (Kotani et al. 2008), or Pup ligase PafA in PUP-IT (Liu et al. 2018). These enzymes are genetically fused to a protein of interest (the *bait*), and generate short-lived intermediate reactive biotins that diffuse away from the bait site and covalently tag neighboring proteins (the *prey*), except in PUP-IT, where the biotin handle does not leave the bait. Other methods of tagging include using photosensitizers such as the enzyme miniSOG (Zhai et al. 2022) or iridium-conjugated antibodies to generate singlet oxygen (Müller et al. 2021) or activated carbenes (Geri et al. 2020), as alternate intermediates for targeting biotin-tagged probes. Subsequently, biotin-tagged prey proteins are enriched using streptavidin-coated beads and identified using mass spectrometry (MS).

BioID is preferred over other PL methods in many *in vitro* and *in vivo* applications, since peroxidases such as APEX and HRP require the addition of hydrogen peroxide and miniSOG produces reactive oxygen species, which can both be toxic to cells. However, BioID has long labeling times (>18 hrs) and requires an optimal temperature of 37° C (Roux et al. 2012). In an effort to improve BioID's performance, TurboID has been introduced as a fast-labeling biotin ligase (10 min labeling time) that also retains activity at temperatures <37° C, which enables it to

be used in organisms like flies, worms, yeast (Branon et al. 2018), and plants (Mair et al. 2019), as well as in cell culture (Shafraz et al. 2020). However, TurboID can biotinylate proteins using endogenous cellular biotin, which creates a large labeling background as well as cellular toxicity. To overcome this limitation, a 'split-TurboID' technology was recently introduced, which splits the TurboID enzyme into two inactive halves that only induce biotinylation when reconstituted by the addition of a chemical cofactor, rapamycin. While this reduces background labelling and increases spatial specificity (Cho et al. 2020), the requirement that both halves of Split-TurboID be expressed in close proximity creates a level of background biotinylation unrelated to the addition of the cofactor (Cho et al. 2020). Additionally, usage of a cofactor introduces the possibility of uncontrolled effects on cellular processes, and the time resolution is limited by the cofactor's ability to diffuse to the cell compartment of interest. Furthermore, the difficulty of removing the factors from the media makes it difficult to control the initiation and cessation of the biotinylation reaction (Klewer et al. 2019).

These limitations in conventional proximity labeling can be overcome by developing new classes of proximity labeling technologies that can be activated on demand without the addition of chemical cofactors, and with high spatial and temporal control. We therefore designed a proximity labeling technology that is precisely triggered without addition of a chemical cofactor, but instead by using blue (488 nm) light. Our system, called Light Activated BioID (LAB), is generated by fusing the two halves of the split-TurboID enzyme to genetically encoded *Arabidopsis thaliana* photodimeric proteins cryptochrome 2 (CRY2) and cryptochrome-interacting basic-helix-loop-helix (CIB1) (Liu et al. 2008). Upon exposure to blue light, CRY2 and CIB1 dimerize within 300 ms (Kennedy et al. 2010, Taslimi et al. 2016) and reconstitute the two halves of the split-TurboID enzyme, thereby inducing biotinylation. Since the photodimers have a half-life of ~6 minutes (Kennedy et al. 2010, Taslimi et al. 2016), dissociation of CRY2 and CIB1 re-splits the TurboID and halts biotinylation. Since LAB dissociates within minutes after the blue light

is turned off, this reduces the background biotinylation and minimizes false positives as well as cellular toxicity due to over-biotinylation.

Here, as a proof of concept, we use live cell imaging, immunofluorescence, western blots, and mass spectrometry (MS) to show in Human Embryonic Kidney (HEK) 293T cells that LAB dimerizes and biotinylates proximal proteins when exposed to blue light. Next, by fusing LAB to the ubiquitous cell-cell adhesion protein E-cadherin (Ecad) in Madin-Darby canine kidney (MDCK) cells, we demonstrate that LAB can identify a protein's known binding partners.

Results:

LAB dimerizes upon blue light illumination: We developed genetically encodable LAB constructs by fusing previously reported low-affinity split-TurboID (L73/G74) (Cho et al. 2020) onto light-inducible dimerizing plant proteins CRY2 and CIB1. The N-terminal fragment of split-TurboID (spTN) and CIB1 were fused onto plasma membrane-targeted enhanced Green Fluorescent Protein (pmEGFP). The C-terminal split TurboID fragment (spTC) and CRY2 were fused onto mCherry and expressed in the cytoplasm (Fig. 1 a). We hypothesized that, upon blue light exposure, CRY2-spTC-mCherry (*henceforth referred to as CryC*) would translocate to the plasma membrane and bind to CIB1-spTN-pmEGFP (*henceforth referred to as CibN*) (Fig. 1 a).

We transiently expressed both constructs in HEK293T cells and observed that CryC was distributed throughout the cytoplasm while CibN was localized at the plasma membrane (Fig. 1 b). When briefly illuminated with a 488 nm laser, CryC translocated to the plasma membrane within seconds of laser exposure and dissociated back to the cytoplasm in ~10 mins (Fig. 1 b). These kinetics show that the fused constructs don't alter the previously reported CRY2/CIB1 kinetics (Kennedy et al. 2010). Furthermore, when a selected region of the plasma membrane

was illuminated with a 488 nm laser, CryC began accumulating in under a second and reached maximum accumulation in seconds (Fig. 1 c, d, e). This demonstrates that LAB can be activated in selected regions of the cell and split-TurboID will be bound for ~ 10 mins from the end of illumination, biotinylating neighboring proteins and giving more temporal and spatial control over previous PL systems.

LAB biotinylates only in the presence of blue light and biotin: Since split-TurboID shows significant biotin labeling after 1hr (Cho et al. 2020), we transiently co-expressed CibN and CryC in HEK cells and exposed the cells to alternating 10-minute cycles of blue light (470 nm) and darkness for 1hr using a blue LED light in the presence of 100 µM biotin (Fig. 2a). We then fixed the cells and stained them for GFP, mCherry, and biotin using anti-GFP and anti-mCherry antibodies and Alexa-647 conjugated streptavidin (Sta) (Fig. 2 b-g, S1-6). Next, we measured the level of Sta on the membrane; Sta fluorescence intensity was normalized to CibN fluorescence intensity to account for differences in CibN expression levels in different cells (Fig. 2 h, S13, table S1). We also quantified the colocalization of CryC and Sta with membrane-bound CibN (Fig. 2 i, table S2). All p-values are catalogued in the supplementary information (tables S3, S4).

In the presence of light and biotin, CryC accumulated at the plasma membrane and caused significant proximal membrane biotinylation (Fig. 2 b, S1), with 69.0 ± 4.7 % Sta fluorescent intensity, compared to significantly lower intensity in other conditions (Fig. 2 h, S13, table S1). CryC and Sta also showed strong colocalization with CibN, with Pearson's coefficients of 0.59 ± 0.02 and 0.57 ± 0.02 respectively (Fig. 2 i, S13, table S2). When samples were kept in darkness, the CryC did not localize to the membrane and no biotinylation was observed (Fig. 2 c, S2), with only a 4.8 ± 0.5 % Sta signal (Fig. 2 h, S13, table S1) and a Pearson's coefficient of 0.15

± 0.03 between CryC and CibN and a Pearson's coefficient of 0.17 ± 0.03 between Sta and CibN (Fig. 2 i, table S2). Similarly, when cells were exposed to light in the absence of biotin, CryC localized with CibN (Pearson's coefficient of 0.59 ± 0.02) (Fig. 2 d, i, S3, S13, table S2), but did not cause significant biotinylation; Sta fluorescent intensity was 1.6 ± 0.1 %, with a 0.09 ± 0.02 Pearson's coefficient between Sta and CibN (Fig. 2 h, i, table S2). Furthermore, in the absence of both light and biotin, no CryC membrane localization (Pearson's coefficient of 0.17 ± 0.03) (Fig. 2 i, table S2) or biotinylation was observed (Fig. 2 e, S4, table S1), with Sta intensity measured at 1.7 ± 0.2 % and a -0.004 ± 0.013 Pearson's coefficient calculated between Sta and CibN (Fig. 2 h, i, S13, table S2). Finally, no biotinylation was measured when only CryC (Fig. 2 f, S5) or CibN (Fig. 2 g, S6) was expressed. Hence, the immunofluorescence data demonstrates that CibN and CryC dimerize and biotinylate only when exposed to blue light.

Ecad-LAB activity is light-dependent: Next, to validate LAB activity with a well-characterized protein and in a different cell line, we fused LAB to the ubiquitous cell-cell adhesion protein E-cadherin (Ecad) in MDCK cells. Ecad plays key roles in the formation and maintenance of epithelial tissues and acts as a tumor suppressor (Xie et al. 2022). We fused CIB1 and spTN onto Ecad-EGFP (ECibN) (Fig. 3 a) and transiently expressed it with CryC in MDCK cells containing endogenous Ecad. Cells were exposed to alternate 10 min cycles of light and darkness for 1hr before fixing and immunostaining.

First, we confirmed that Ecad-CibN localizes to cell-cell junctions (Fig. 3 b, S7-S12). Next, cells were exposed to blue light and biotin, and CryC accumulation at the junction was monitored. To measure biotinylation, Sta fluorescence intensity (normalized by ECibN fluorescence intensity to account for variation in ECibN expression levels) was measured. The Sta fluorescence intensity

of 24.7 ± 1.8 % near the membrane confirmed biotinylation activity, with a measured colocalization coefficient of 0.54 ± 0.02 for ECibN and Sta and 0.49 ± 0.02 for ECibN and CryC (Fig. 3 b, h, i, S 7, table S5, S6). In the absence of light and the presence of exogenous biotin, CryC did not colocalize with ECibN (Pearson's coefficient 0.13 ± 0.02) (Fig. 3 c, S8, table S6), and no biotinylation was detected, with a Sta intensity of 4.8 ± 0.4 % and a Pearson's coefficient of 0.06 ± 0.01 for ECibN and Sta (Fig. 3 c, h, i, S8, table S5, S6), indicating biotinylation is light dependent. Furthermore, when cells were illuminated with blue light in the absence of biotin, even though ECibN and CryC showed colocalization with a Pearson's coefficient of 0.4 ± 0.03 (Fig. 3 d, i, S9, table S6), the relative Sta intensity and colocalization was not significant (4.3 ± 0.4% and Pearson's coefficient of 0.03 ± 0.02) (Fig. 3 d, h, i, table S5, S6), demonstrating the absence of biotinylation. Similarly, in the absence of both light and biotin, ECibN/CryC did not colocalize (Pearson's coefficient 0.12 ± 0.02) (Fig. 3 e, i, S10, table S6) or show a substantial Sta signal (4.6 ± 0.4 %) with no colocalization between ECibN and Sta (Pearson's coefficient 0.02 ± 0.01) (Fig. 3 e, h, i, S10, table S6). Finally, when only CryC (Fig. 3 f, S11) or ECibN (Fig. 3 g, S12) was expressed, there was no biotinylation observed. Thus, the immunofluorescence data for ECibN and CryC in MDCK cells confirm that LAB can be applied to other proteins of interest and that when exogenous biotin is provided, its biotinylation activity depends only on exposure to light. All p-values are catalogued in supplementary information (tables S7, S8).

Western blot shows light-dependent biotinylation: To further characterize LAB, we performed western blots on HEK and MDCK cells and stained for biotinylation. CryC was transiently co-expressed with CibN in HEK cells and with ECibN in MDCK cells. Cells were exposed to blue light in the presence of biotin for 10 min on/off intervals for 1 hr for HEK cells and 4 hr for MDCK cells. To compare biotinylation efficiency of LAB in HEK cells, we transiently

expressed a full TurboID construct (CIB1-TurboID-pmEGFP) and incubated in 100 µM biotin for 1 hr. The cells were then lysed and biotinylated proteins were captured using streptavidin-conjugated beads and used for western blots, with the eluted protein stained with Sta-HRP (Fig. 4 a, b, S14 A). Western blots showed significantly higher biotinylation in light-exposed HEK293T cells compared to cells kept in darkness and less biotinylation than cells expressing TurboID, which could be due to a lower background from LAB (Fig. 4a, S14 A). MDCK cells (Fig. 4 b) also showed significantly higher biotinylation in the presence of light, confirming the light-dependent activity of LAB.

While we did not have any known prey for CibN in HEK293T cells, we expected the GFP and mCherry portions of CibN and CryC to be biotinylated, as these would be directly proximal to the reconstituted Split-TurboID. When we stained eluted protein with GFP and mCherry antibodies, we found a much higher presence of these proteins in the light-positive condition than the light negative, with no staining occurring on a blank control (Fig. S14 b, c). Previous TurboID studies show that the cytoplasmic region of Ecad binds to β-catenin adaptor proteins (Guo et al. 2014, Shafraz et al. 2020). In agreement with previous studies, our western blot data showed that in MDCK cells, both Ecad (Fig. 4 c) and β-catenin (Fig. 4 d), were biotinylated. The western blot data also showed a greater level of biotinylated endogenous Ecad and ECibN in light exposed MDCK cells (Fig. 4 c). Additionally, β-catenin was found only in the light-exposed sample (Fig. 4 d), showing that LAB biotinylates proximal proteins in a light-dependent manner and identifies expected binding partners.

MS data for HEK identifies expected proteins: After confirming LAB's activity with immunofluorescence and western blots, we used MS to identify proximal biotinylated proteins

using CibN and CryC constructs in HEK293T cells (it was not possible to conduct MS analysis in MDCK cells since the expression levels of transiently transfected ECibN and CryC were very low). HEK cells transiently co-expressing CibN and CryC were exposed to blue light for 1 hr using 10 min on/off cycles in the presence of biotin while control cells were kept in darkness, also in the presence of biotin. The biotinylated proteins were then captured using streptavidin-coated magnetic beads and trypsin digested before LC-MS/MS was performed for three replicates per condition to identify the biotinylated proteins. MS data showed significant enrichment of proteins in cells illuminated with blue light compared to those kept in darkness (Fig. 4 e). CIB1 and GFP, which are close to the Split-TurboID, are expected to be biotinylated and were significantly enriched as expected (Fig. 4 e). Finally, principal component analysis (PCA) showed two separate clusters for the light-exposed samples and the controls, implying distinctive variations between both groups (Fig. 4 f).

Discussion:

For LAB, we used split-TurboID as the labeling enzyme due to its extensively characterized biotinylation kinetics. Similarly, we used the photodimer pair, CRY2 and CIB1, since they are one of the most widely-used photodimer systems and have been tested in many different cell lines as well as in living organisms to investigate a wide variety of cellular functions (Taslimi et al. 2016). Importantly, CRY2/CIB1 binding kinetics complement those of Split-TurboID by remaining associated long enough after light exposure to allow for sufficient biotinylation while not remaining bound too long post-exposure so that the labelling reaction can be arrested with the removal of light.

Using immunofluorescence, western blots, and MS, in both HEK293T and MDCK cells, we demonstrated that LAB can be selectively activated through researcher-controlled biotin and

light application. LAB's specificity was validated through the light exposure dependent detection of β-catenin, which is known to be associated with Ecad in MDCK cells (Shafraz et al. 2020). Importantly, β-catenin was absent in the light negative condition, showing that LAB successfully labels proximal proteins to the bait protein in a light-dependent manner. Additionally, the populations of proteins detected via MS, with and without light in HEK293T cells, were significantly different both in the specific proteins that were biotinylated, and their amounts.

A consideration when using LAB is cell-line dependent differences in LAB light sensitivity and efficiency of transient expression. For example, we found that LAB expressed in HEK293T cells has a higher expression and light sensitivity compared to MDCK cells. Additionally, low expression levels in MDCK cells resulted in low CryC membrane recruitment, which made quantification of membrane CRY2 intensity difficult. In contrast, in HEK293T cells, where transient LAB expression was more efficient, changes in CryC fluorescence intensity relative to CibN fluorescence intensity were light dependent (Fig. S13). However, despite the low ECibN transfection efficiency in MDCK cells, the pattern of Sta intensity changes in these cells was consistent with what we observed in HEK293T cells. Taken together with colocalization analysis under different conditions, our results convincingly demonstrate that LAB can be reliably used across different cell lines. We anticipate that the issues that arise from low transient expression levels of LAB can be mitigated via generation of stable cell lines. Furthermore, truncated versions of the CRY2 and CIB1 proteins have been developed (Taslimi et al. 2016), that can be used in LAB if large constructs would affect expression and localization of bait proteins tagged with LAB.

Recently, a different opto-dimerization system, iLID, has been used with a new split-TurboID variant (Chen et al. 2022). However, iLID has a half-life of under a minute (Kennedy et al. 2010, Taslimi et al. 2016), which may not provide enough time for appreciable labeling to occur before the dimers unbind and inactivate Split-TurboID. Furthermore, in this opto-dimerization

study, TurboID was split at a previously uncharacterized location (G99/E100) and consequently, the rate of biotinylation of this new split-TurboID variant is unknown (Chen et al. 2022).

Another PL tool using light-activated miniSOG has been recently developed (PDPL), which uses singlet oxygen to create electrophilic residues on prey proteins, which can be subsequently bound to an alkyne chemical probe and pulled down using click chemistry (Zhai et al. 2022). However, the aniline probe used with PDPL can be toxic to cells (Wang et al. 2016, Zhai et al. 2022). Furthermore, miniSOG has a labeling radius of up to 70nm, which is much larger than TurboID's 10nm labelling radius (Kim et al. 2014). While a smaller labeling radius is more suited for discovering direct PPIs, a larger labeling radius is more appropriate for identifying proteins that may be present in the same cellular compartment (Cho et al. 2020, Zhai et al. 2022). Another light-activated PL tool, MicroMap, which uses an antibody conjugated to an iridium photocatalyst to label nearby proteins via carbene intermediates, has also recently been developed (Geri et al. 2020, Seath et al. 2021). However, the necessity of a primary antibody that binds to the bait protein at a convenient location limits MicroMap's applications.

It has previously been shown that CRY2 can homodimerize when illuminated with blue light (Wang et al. 2020). However, this is not an issue for LAB since our construct only has the inactive C-terminus of Split-TurboID associated with CRY2. Consequently, CRY2 homodimerization cannot reconstitute a functional TurboID. As a result, no biotinylation is observed in the CryC-only condition (Fig. 2 f). Moreover, CRY2 homodimerization does not prevent interaction with CIB1.

Unlike CRY2 and CIB1, which photodimerize in the presence of blue light, photodimerization activated by longer wavelength light could be more effective for PPI identification in deeper tissue. However, the two known red light activated photodimers (PhyB/PIF3 and PhyB/PIF6), require light exposure at different wavelengths for both activation

and inactivation (Klewer et al. 2019). We therefore chose a photodimer pair that dissociated in the dark, rather than through alternate wavelength exposure, for ease of use. Importantly, since CRY2/CIB1 dimerization can be triggered using two-photon excitation (Kennedy et al. 2010), this may allow LAB to map PPIs in deeper tissue *in vivo*.

We anticipate that the ability to activate LAB using light, coupled with its high temporal resolution, can be exploited to interrogate differences in PPIs at different time points in the cell cycle. We also expect that by using focused activating light, LAB can be used to identify differences in PPI at distinct cellular locations. Finally, like TurboID, which has previously been used to map extracellular PPIs (Shafraz et al. 2020), we anticipate that LAB can also be used to investigate extracellular protein interactions with high spatial and temporal resolution.

Materials and Methods:

Cloning of plasmid constructs: CibN was generated by restriction digesting a CIB-pmEGFP plasmid (Addgene plasmid # 28240, (Kennedy et al. 2010)) at AgeI and NheI sites and fusing PCR amplified CIB1 and spTN (Addgene plasmid # 153002, (Cho et al. 2020)) using Gibson assembly. SpTN was connected to CIB1 and pmEGFP with linkers V5-KGSGSTSGSGTG (Linker 1) and GSGPVAT. CryC was constructed by inserting PCR amplified spTC (Addgene plasmid #153003, (Cho et al. 2020)) onto restriction-digested Cry2-mCherry (Addgene plasmid # 26871, (Kennedy et al. 2010)) at XmaI sites with linkers ARGKGSGSTSGSG and KGSGDPPVAT.

To design ECibN, first V5-spTN-CIB-pmEGFP was constructed by restriction digesting CIB1-pmEGFP with NheI and inserting PCR amplified Linker1-spTN-KGSGAT. Then, Ecad-EGFP plasmid was restriction digested at NotI and XhoI sites and EGFP was reintroduced without

the stop codon. Next, NotI and HindIII sites of Ecad-EGFP were restriction digested and PCR amplified V5-spTN-CIB was inserted using Gibson assembly. Ecad-EGFP plasmid was a kind gift from Prof. Soichiro Yamada at the University of California, Davis. All enzymes were high efficiency enzymes from New England Biolabs. All primers used are listed in SI (table S9).

Cell culture and transfection: HEK293T cells were grown in High Glucose (4.5 g/L) Dulbecco's modified Eagle's medium (DMEM, Gibco) cell culture media with 10% fetal bovine serum (Gibco) and 1% Penicillin-Streptomycin (PSK) (10,000 U/mL, Life Technologies). MDCK cells were cultured in Low Glucose (1 g/L) DMEM (Gibco) cell culture media with 10% fetal bovine serum and 1% PSK.

HEK cells were transfected at 80% confluency with CibN and CryC plasmids while MDCK cells were transfected with ECibN and CryC at 30% confluency. For live cell imaging and immunofluorescence and for MDCK western blots, Lipofectamine 3000 (Invitrogen) was used for transfection following the manufacturer's protocol. For HEK in p150 dishes, plasmids were transfected with polyethylenimine (PEI) (Polysciences, Inc.). Plasmids and PEI were diluted in Opti-MEM (Gibco) at a 1µg:5µg DNA:PEI ratio. After five minutes, both solutions were mixed and incubated for 90 min and then added to the cells.

Live cell imaging: HEK cells were imaged >12 h post-transfection using a 561 nm laser to visualize mCherry and a 488 nm laser to image EGFP and to photo-excite CryC. Images were reconstructed using ImageJ. For the intensity profile of CryC accumulation, a 1µm line was drawn across a selected membrane region and the raw pixel intensity across the line was plotted (Fig. 1 c). Measurements were taken using ImageJ's Plot Profile analysis feature. To plot CryC accumulation over time, a 0.225µm by 0.900µm box was drawn on the cell membrane bracketing the intensity profile line (Fig. 1 c). Measurements for each frame were taken using ImageJ's ROI mean intensity measurement capability.

Immunofluorescence: After more than 12 hrs post-transfection, cells were transferred to FluoroBrite DMEM (Gibco) with 10% FBS and 1% PSK. Then, cells were incubated with 100 µM biotin and exposed to blue light in 10 min intervals for 1 hr using blue LED light source (Blue box Pro Transilluminator, miniPCR bio). Control cells were kept in dark. Then, cells were immediately fixed using 3% paraformaldehyde and 0.3% Triton X-100 in phosphate-buffered saline (PBS) for 10 min and blocked with 1% bovine serum albumin (BSA) and 0.3% Triton X-100 in PBS for 30 min. Anti-GFP antibody (rabbit polyclonal, Rockland Immunochemicals) and Alexa Fluor 488-conjugated Goat anti-rabbit antibody (Life Technologies) were used to detect GFP-tagged proteins. Anti-mCherry (mouse monoclonal, Invitrogen) and Alexa Fluor 568-conjugated Goat anti-mouse antibody (Invitrogen) were used to detect mCherry. Biotinylated proteins were identified with Alexa Fluor 647-conjugated streptavidin (Invitrogen). Primary antibodies were incubated for 1 hr (1:1000 dilution in PBS with 1% BSA and 0.3% Triton X-100) and secondary antibodies were incubated for 30 min (1:1000 dilution in PBS with 1% BSA and 0.3% Triton X-100). Cells were imaged using a Leica Microsystems Stellaris 5 confocal setup with 63x/1.40 NA oil objective. Images were reconstructed using ImageJ.

Image analysis: All analysis was done in ImageJ. In order to reduce background and oversaturated pixel contribution, all images were processed with a Gaussian filter with a sigma of 11 (HEK images) or 10 (MDCK images). The filtered image was then subtracted from the original image, and membrane ROIs were hand-chosen with the wand tool from the CibN / ECibN GFP channel using a threshold minimum of 50 (HEK images) or 30 (MDCK images) on the Threshold tool. Lower Gaussian sigmas and thresholds were used on MDCK cells due to the lower expression of ECibN. The ROIs were used for both fluorescence intensity measurements and colocalization analysis. Colocalization analysis was carried out on the processed images using the Coloc2 plugin with Costes threshold regression, a PSF of 3, and 10 Costes randomizations. Unthresholded Pearson's coefficients were used from the outputs. Intensity measurements for all

channels were taken on the processed images using the Multi Measure functionality on the ROI manager.

Purification of biotinylated proteins for western blot and MS analysis: CibN and CryC were transiently expressed in HEK cells and ECibN and CryC in MDCK cells cultured on p150 dishes. The next day, the cells were incubated with 100 μM biotin and exposed to blue light on a 10 min on/off cycle for 1 hr (HEK) or 4 hrs (MDCK). Control cells were kept in darkness. After incubation, cells were washed three times with PBS, scraped and centrifuged. Pelleted cells were resuspended in lysis buffer (50 mM Tris pH 7.5, 150 mM NaCl, 0.4% sodium dodecyl sulfate (SDS), 1% octyl phenoxy poly(ethyleneoxy) ethanol (IGEPAL CA-630), 1.5 mM $MgCl_2$, 1 mM EGTA) with 2 μL/mL of protease inhibitor mixture (Sigma-Aldrich), and 1 μL/mL Benzonase Nuclease (250 U/μL) (Millipore-Sigma). The lysate was flash frozen in dry ice and quickly thawed at 37 °C. Then, the lysate was incubated for 30 min at 4 °C and sonicated at 30% duty ratio for 1 min. Next, the lysate was centrifuged at 13,000 rpm for 30 min at 4 °C. After that, the concentrations of the supernatant were measured with an RC DC protein assay kit (Bio-Rad). Concentration of the supernatant was normalized to the lowest concentration and lysis buffer was added to bring all volumes to 1mL. Supernatant was incubated with 50 μL of superparamagnetic streptavidin conjugated beads (Dynabeads MyOne Streptavidin C1, Invitrogen) and rotated overnight at 4 °C. The next day, beads were washed with the lysis buffer. Then, beads were washed with the 2% SDS in 50 mM Tris, pH 7.4, and twice with lysis buffer.

For the western blots, after capturing the biotinylated proteins, beads were incubated with 60 μl of 2.5 mM biotin at 95 °C for 5 min. Then, the eluted biotinylated proteins were collected and run on a 4-15% Mini-Protean TGX Precast Protein Gel (Bio-Rad) before being transferred to a nitrocellulose membrane and stained for biotin using Sta conjugated with Horseradish Peroxidase (HRP) (1:1000 dilution, Invitrogen). To detect Ecad and β-catenin in MDCK cells,

mouse anti-Ecad antibody (1:1000, BD Biosciences) and mouse anti-β-catenin antibody (1:1000, BD Biosciences) were used as primary antibodies. HRP conjugated goat anti-mouse was used as secondary antibody (1:1000, Invitrogen). WesternBright ECL HRP substrate (Advansta) was used to detect the protein. Images were acquired using Image Lab software from Bio-Rad.

For MS, after the incubation and 2% SDS Tris and lysis buffer wash steps, magnetic beads were then washed three times with 50 mM ammonium bicarbonate (NH_4HCO_3) and resuspended in 60 µL of 50 mM NH_4HCO_3 containing 5 µg of trypsin for overnight digestion at 37 °C in a shaker. The resulting peptides were recovered from the beads by removing the supernatant after pelleting the beads via magnetic holder, and tryptic peptides from the supernatant were dried in a vacuum centrifuge and reconstituted in 0.1% formic acid. Tryptic peptides were analyzed using nano-scale liquid chromatographic tandem mass spectrometry (nLC-MS/MS). Three replicates of each condition were used.

Mass Spectrometry: For each sample, an equal volume of peptide was loaded onto a disposable Evotip C18 trap column (Evosep Biosystems, Denmark) as per the manufacturer's instructions. Briefly, Evotips were wetted with 2-propanol, equilibrated with 0.1% formic acid, and then loaded using centrifugal force at 1200 g. Evotips were subsequently washed with 0.1% formic acid, and then 200 µL of 0.1% formic acid was added to each tip to prevent drying. The tipped samples were subjected to nanoLC on an Evosep One instrument (Evosep Biosystems). Tips were eluted directly onto a PepSep analytical column, dimensions: 8cm x 150µm, C18 column with 1.5 µm particle size (PepSep, Denmark), and a ZDV spray emitter (Bruker Daltronics). Mobile phases A and B were water with 0.1% formic acid (v/v) and 80/20/0.1% ACN/water/formic acid (v/v/vol), respectively. The standard pre-set method of 60 samples-per-day was used, which is a 26 min gradient.

Mass spectrometry was performed on a hybrid trapped ion mobility spectrometry-quadrupole time of flight mass spectrometer (timsTOF Pro, Bruker Daltonics) with a modified nano-electrospray ion source (CaptiveSpray, Bruker Daltonics), as described previously (Shafraz et al. 2020). Mass spectrometry raw files were processed with MsFragger (Yu et al. 2020) as previously described (Shafraz et al. 2020). Volcano and PCA plots were generated using Spectronaut viewer. Known contamination proteins (Hodge et al. 2013) were removed and a background signal was added for genes that didn't have enough signal for quantification (using background signal imputation method, where the software chooses the best background signal to report as the precursor quantity). This allowed protein concentrations to be compared between the light positive and light negative conditions and ameliorated issues where proteins at too low concentrations in the negative condition could not be compared to the light positive condition.

Acknowledgements: This research was supported in part by the National Institute of General Medical Sciences of the National Institutes of Health (R01GM121885) and the National Science Foundation (MCB-2022385). We thank Dr. Gabriela Grigorean for performing LC-MS/MS and data analysis in Proteomics Core Facility of the Genome Center at University of California, Davis.

Author contributions: O.S. and S.S. designed research; O.S. and C.M.O.D. collected and analyzed data; and O.S., C.M.O.D., and S.S. wrote the paper.

Figure Legends

Figure 1: Light Activated BioID (LAB). (a) Schematic of LAB construct used in HEK293T cells. Fragment of Split-TurboID (N) and *Arabidopsis* protein CIB1 were fused onto prenylated plasma membrane targeted Enhanced Green Fluorescent Protein (pmEGFP) that localizes to the plasma membrane (CibN). The complementary Split-TurboID (C) fragment was fused to blue-light receptor protein Cryptochrome 2 (CRY2) and mCherry fluorescent protein (CryC) and expressed in the cytoplasm. When exposed to blue light, CRY2 interacts with CIB1 and reconstitutes the split-TurboID, which generates reactive biotin for proximity labeling. Both constructs were co-expressed in HEK293T cells. (b) Confocal images show CibN localizing to the membrane and CryC diffused in the cytoplasm of the cells. When excited with a 488 nm laser, CryC localized to the membrane in seconds and dissociated completely in about 600 sec. Scale bar 3 µm. (c) A region of the membrane was excited with 488 nm laser and CryC accumulation was monitored. CryC accumulated at the membrane region in sub-seconds. Scale bar 3 µm. (d) CryC and CibN intensity was measured across the yellow line in *(c)* with vertical black dashed lines delineating the membrane on the graph. The fluorescence intensity measurements showed strong correlation between CryC and CibN after light exposure. (e) Integrated CryC (red) and CibN (green) intensity was measured in the yellow box in *(c)* over time, with the vertical black dashed line indicating 488 nm laser excitation. CryC fluorescence reached the maximum intensity within seconds, while CibN fluorescence remained constant.

Figure 2: Immunofluorescence imaging shows light-dependent biotinylation. CibN and CryC were transiently co-expressed in HEK 293T cells and, in the presence of 100 µM biotin, were exposed to 10 min cycles of alternating blue light and darkness for 1hr. The cells were fixed

and stained for EGFP, mCherry, and biotin. (a) Schematic of light exposure sequence used. (b) Immunofluorescence showed that in the presence (+) of exogenous biotin and light, membrane-localized CibN (EGFP) and CryC (mCherry) dimerized and biotinylated proteins (Streptavidin, Sta) in the vicinity of the plasma membrane, with composite images confirming the colocalization of CibN, CryC, and Sta. In the absence (-) of blue light (c), in the absence of added biotin (d), or in the absence of both biotin and light (e), no biotinylation was observed. When only CryC (f) or CibN (g) were expressed, no biotinylation was detected, showing CibN and CryC dimerization are essential for proximity labeling. To facilitate an unbiased visual comparison of fluorescence intensities in (*b* - *g*), the panels in each column display identical minimum and maximum intensities. (h) Bar graph of Sta fluorescent intensity averaged across number of cells show significant biotinylation occurring only in the presence of light and biotin. Fluorescent intensity of Sta proximal to membrane region was normalized to CibN to account for variation in CibN expression levels in different cells. Normalized fluorescence intensities are tabulated in table S1 while corresponding p-values are tabulated in table S3. (i) Average Pearson's coefficient shows CibN and CryC colocalize in the presence of light, while Sta colocalizes to CibN only in the presence of light and biotin. Average Pearson's coefficient values are tabulated in table S2 while corresponding p-values are tabulated in table S4. All scale bars 10 µm. Errors: s.e. n= # of cells.

Figure 3: Ecad-CibN and CryC dimerize and biotinylate only when exposed to light. Ecad-EGFP fused with Split-TurboID(N) and CIB1 (ECibN) and CryC were co-expressed transiently in MDCK cells. Cells incubated with 100 µM biotin were illuminated with blue light, for an hour, on a 10 min on/off cycle. The cells were fixed and stained for EGFP, mCherry and biotin. (a) Schematic of LAB fused with Ecad. EGFP, fragment of Split-TurboID (N), and CIB1 were fused onto the C terminus of Ecad to create ECibN. CryC was expressed in the cytoplasm. Both

constructs were co-expressed in MDCK cells. (b) ECibN localizes to the intercellular junction, and in the presence (+) of light and biotin, CryC translocates to the membrane and dimerizes, which results in the biotinylation of proteins closer to the membrane, which is confirmed with composite images showing the colocalization of CibN, CryC, and Sta. In the absence (-) of light (c), biotin (d), or both (e), biotinylation is not observed. When only CryC (f) or ECibN (g) were expressed, no biotinylation was observed. To facilitate an unbiased visual comparison of fluorescence intensities in (*b* - *g*), the panels in each column display identical minimum and maximum intensity. (h) Fluorescent intensity of Sta normalized to ECibN intensity to account for variation in expression levels in different cells shows that biotinylation is detected only in the presence of light and biotin. Normalized fluorescence intensities are tabulated in table S5 while corresponding p-values are tabulated in table S7. (i) Average Pearson's coefficient shows ECibN and CryC colocalize in the presence of light, while Sta colocalizes to ECibN only in the presence of light and biotin. Average Pearson's coefficient values are tabulated in table S6 while corresponding p-values are tabulated in table S8. All scale bars 10 µm. Errors: s.e. n= # of cells.

Figure 4: Western blots and mass spectrometry (MS) analysis for LAB. (a) Western blot of CibN and CryC expressed in HEK293T cells, incubated with 100 µM biotin, stained for biotinylation with Sta-HRP. Cells exposed to blue light for an hour on a 10 min on/off cycle show a greater Sta-HRP signal, compared to cells kept in dark. (b-d) ECibN and CryC were co-expressed in MDCK cells with 100 µM added biotin, exposed to blue light for four hours on a 10 min on/off cycle, and stained for biotinylation, Ecad, and β-catenin. Light-exposed cells show greater light-dependent biotinylation determined by Sta-HRP compared to those kept in the dark (b), and demonstrate biotinylation of ECibN and endogenous Ecad (EcadWT) (c), and β-catenin, an adaptor protein known to interact with Ecad cytoplasmic region (d). (e) MS data for HEK293T

cells show more biotinylated proteins for light-exposed cells (cyan) compared to cells kept in dark (magenta), with CIB1 and GFP (circled) being among the top-ranked in the data. (f) Principal Component Analysis (PCA) shows similar variation for all replicates of the same condition (R1, R2, R3), with light-exposed cells (cyan) calculated to be significantly different from the control cells kept in the dark (magenta) with 100 µM added biotin.

References:

Branon, T. C., J. A. Bosch, A. D. Sanchez, N. D. Udeshi, T. Svinkina, S. A. Carr, J. L. Feldman, N. Perrimon and A. Y. Ting (2018). "Efficient proximity labeling in living cells and organisms with TurboID." Nat Biotechnol **36**(9): 880-887.

Chen, R., N. Zhang, Y. Zhou and J. Jing (2022). "Optical Sensors and Actuators for Probing Proximity-Dependent Biotinylation in Living Cells." Frontiers in Cellular Neuroscience **16**.

Cho, K. F., T. C. Branon, S. Rajeev, T. Svinkina, N. D. Udeshi, T. Thoudam, C. Kwak, H.-W. Rhee, I.-K. Lee, S. A. Carr and A. Y. Ting (2020). "Split-TurboID enables contact-dependent proximity labeling in cells." Proceedings of the National Academy of Sciences **117**(22): 12143-12154.

Cho, K. F., T. C. Branon, N. D. Udeshi, S. A. Myers, S. A. Carr and A. Y. Ting (2020). "Proximity labeling in mammalian cells with TurboID and split-TurboID." Nature Protocols **15**(12): 3971-3999.

Choi-Rhee, E., H. Schulman and J. E. Cronan (2004). "Promiscuous protein biotinylation by Escherichia coli biotin protein ligase." Protein Science **13**(11): 3043-3050.

Geri, J. B., J. V. Oakley, T. Reyes-Robles, T. Wang, S. J. McCarver, C. H. White, F. P. Rodriguez-Rivera, D. L. Parker, Jr., E. C. Hett, O. O. Fadeyi, R. C. Oslund and D. W. C. MacMillan (2020). "Microenvironment mapping via Dexter energy transfer on immune cells." Science **367**(6482): 1091-1097.

Guo, Z., L. J. Neilson, H. Zhong, P. S. Murray, S. Zanivan and R. Zaidel-Bar (2014). "E-cadherin interactome complexity and robustness resolved by quantitative proteomics." Sci Signal **7**(354): rs7.

Hodge, K., S. T. Have, L. Hutton and A. I. Lamond (2013). "Cleaning up the masses: exclusion lists to reduce contamination with HPLC-MS/MS." Journal of Proteomics **88**: 92-103.

Kennedy, M. J., R. M. Hughes, L. A. Peteya, J. W. Schwartz, M. D. Ehlers and C. L. Tucker (2010). "Rapid blue-light-mediated induction of protein interactions in living cells." Nature Methods **7**(12): 973-975.

Kim, D. I., K. C. Birendra, W. Zhu, K. Motamedchaboki, V. Doye and K. J. Roux (2014). "Probing nuclear pore complex architecture with proximity-dependent biotinylation." Proceedings of the National Academy of Sciences of the United States of America **111**(24): E2453-2461.

Kim, D. I., S. C. Jensen, K. A. Noble, B. Kc, K. H. Roux, K. Motamedchaboki and K. J. Roux (2016). "An improved smaller biotin ligase for BioID proximity labeling." Molecular Biology of the Cell **27**(8): 1188-1196.

Klewer, L. and Y.-W. Wu (2019). "Light-Induced Dimerization Approaches to Control Cellular Processes." Chemistry – A European Journal **25**(54): 12452-12463.

Kotani, N., J. Gu, T. Isaji, K. Udaka, N. Taniguchi and K. Honke (2008). "Biochemical visualization of cell surface molecular clustering in living cells." Proceedings of the National Academy of Sciences **105**(21): 7405-7409.

Liu, H., X. Yu, K. Li, J. Klejnot, H. Yang, D. Lisiero and C. Lin (2008). "Photoexcited CRY2 Interacts with CIB1 to Regulate Transcription and Floral Initiation in Arabidopsis." Science **322**(5907): 1535-1539.

Liu, Q., J. Zheng, W. Sun, Y. Huo, L. Zhang, P. Hao, H. Wang and M. Zhuang (2018). "A proximity-tagging system to identify membrane protein-protein interactions." Nature Methods **15**(9): 715-722.

Mair, A., S.-L. Xu, T. C. Branon, A. Y. Ting and D. C. Bergmann (2019). "Proximity labeling of protein complexes and cell-type-specific organellar proteomes in Arabidopsis enabled by TurboID." eLife **8**: e47864.

Martell, J. D., T. J. Deerinck, Y. Sancak, T. L. Poulos, V. K. Mootha, G. E. Sosinsky, M. H. Ellisman and A. Y. Ting (2012). "Engineered ascorbate peroxidase as a genetically encoded reporter for electron microscopy." Nature Biotechnology **30**(11): 1143-1148.

Müller, M., F. Gräbnitz, N. Barandun, Y. Shen, F. Wendt, S. N. Steiner, Y. Severin, S. U. Vetterli, M. Mondal, J. R. Prudent, R. Hofmann, M. van Oostrum, R. C. Sarott, A. I. Nesvizhskii, E. M. Carreira, J. W. Bode, B. Snijder, J. A. Robinson, M. J. Loessner, A. Oxenius and B. Wollscheid (2021). "Light-mediated discovery of surfaceome nanoscale organization and intercellular receptor interaction networks." Nature Communications **12**(1): 7036.

Qin, W., K. F. Cho, P. E. Cavanagh and A. Y. Ting (2021). "Deciphering molecular interactions by proximity labeling." Nature Methods **18**(2): 133-143.

Ramanathan, M., K. Majzoub, D. S. Rao, P. H. Neela, B. J. Zarnegar, S. Mondal, J. G. Roth, H. Gai, J. R. Kovalski, Z. Siprashvili, T. D. Palmer, J. E. Carette and P. A. Khavari (2018). "RNA–protein interaction detection in living cells." Nature Methods **15**(3): 207-212.

Roux, K. J., D. I. Kim, M. Raida and B. Burke (2012). "A promiscuous biotin ligase fusion protein identifies proximal and interacting proteins in mammalian cells." The Journal of Cell Biology **196**(6): 801-810.

Seath, C. P., A. D. Trowbridge, T. W. Muir and D. W. C. MacMillan (2021). "Reactive intermediates for interactome mapping." Chemical Society Reviews **50**(5): 2911-2926.

Shafraz, O., B. Xie, S. Yamada and S. Sivasankar (2020). "Mapping transmembrane binding partners for E-cadherin ectodomains." Proceedings of the National Academy of Sciences **117**(49): 31157-31165.

Taslimi, A., B. Zoltowski, J. G. Miranda, G. P. Pathak, R. M. Hughes and C. L. Tucker (2016). "Optimized second-generation CRY2-CIB dimerizers and photoactivatable Cre recombinase." Nature Chemical Biology **12**(6): 425-430.

Wang, Q. and C. Lin (2020). "A structural view of plant CRY2 photoactivation and inactivation." Nature Structural & Molecular Biology **27**(5): 401-403.

Wang, Y., H. Gao, X.-L. Na, S.-Y. Dong, H.-W. Dong, J. Yu, L. Jia and Y.-H. Wu (2016) "Aniline Induces Oxidative Stress and Apoptosis of Primary Cultured Hepatocytes." International Journal of Environmental Research and Public Health **13** DOI: 10.3390/ijerph13121188.

Xie, B., A. Maker, A. V. Priest, D. M. Dranow, J. N. Phan, T. E. Edwards, B. L. Staker, P. J. Myler, B. M. Gumbiner and S. Sivasankar (2022). "Molecular mechanism for strengthening E-cadherin adhesion using a monoclonal antibody." Proceedings of the National Academy of Sciences **119**(32): e2204473119.

Yu, F., S. Haynes, G. C. Teo, D. Avtonomov, D. Polasky and A. Nesvizhskii (2020). Fast quantitative analysis of timsTOF PASEF data with MSFragger and IonQuant, bioRxiv.

Zhai, Y., X. Huang, K. Zhang, Y. Huang, Y. Jiang, J. Cui, Z. Zhang, C. K. C. Chiu, W. Zhong and G. Li (2022). "Spatiotemporal-resolved protein networks profiling with photoactivation dependent proximity labeling." Nature Communications **13**(1): 4906.

Figure 1

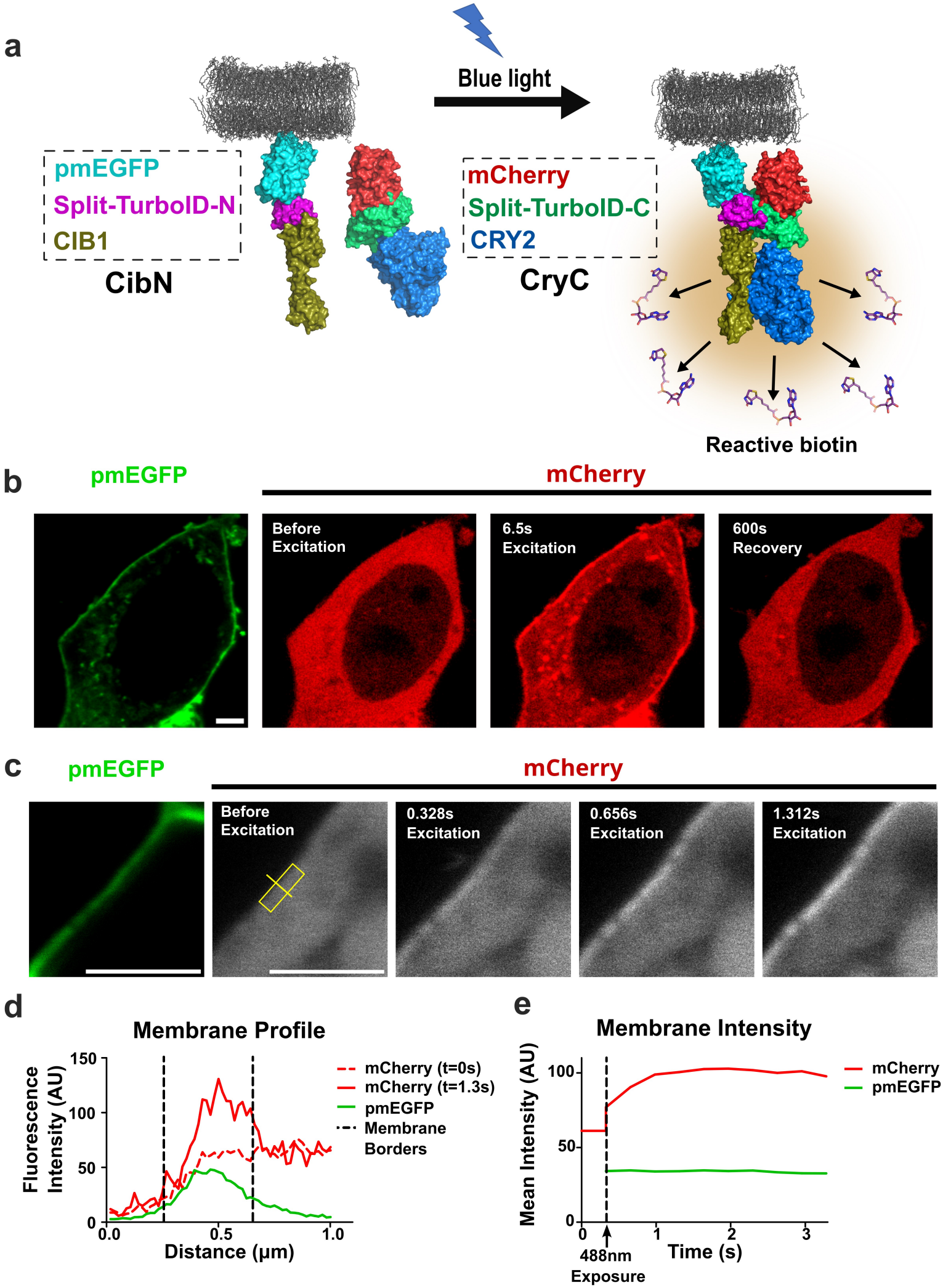
a
Blue light
pmEGFP
Split-TurboID-N
CIB1
CibN
mCherry
Split-TurboID-C
CRY2
CryC
Reactive biotin
b
pmEGFP
mCherry
Before Excitation
6.5s Excitation
600s Recovery
c
pmEGFP
mCherry
Before Excitation
0.328s Excitation
0.656s Excitation
1.312s Excitation
d
Membrane Profile
Fluorescence Intensity (AU)
150
100
50
0
0.0
0.5
1.0
Distance (µm)
mCherry (t=0s)
mCherry (t=1.3s)
pmEGFP
Membrane Borders
e
Membrane Intensity
Mean Intensity (AU)
100
50
0
0
1
2
3
Time (s)
488nm Exposure
mCherry
pmEGFP

Figure 2

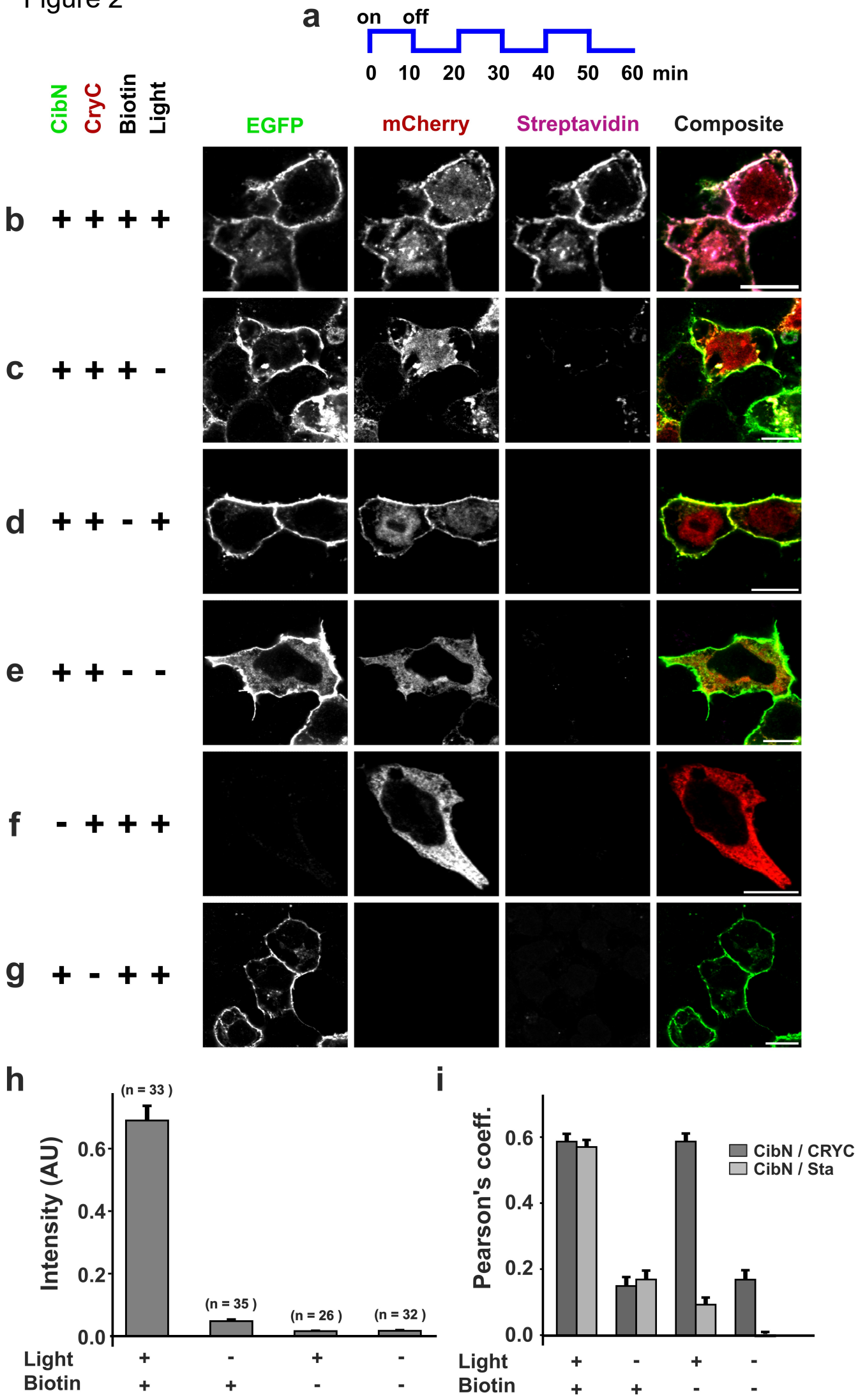
a
on
off
0
10
20
30
40
50
60
min
CibN
CryC
Biotin
Light
EGFP
mCherry
Streptavidin
Composite
b + + + +
c + + + -
d + + - +
e + + - -
f - + + +
g + - + +
h
Intensity (AU)
0.0
0.2
0.4
0.6
(n = 33)
(n = 35)
(n = 26)
(n = 32)
Light + - + -
Biotin + + - -
i
Pearson's coeff.
0.0
0.2
0.4
0.6
CibN / CRYC
CibN / Sta
Light + - + -
Biotin + + - -

Figure 3

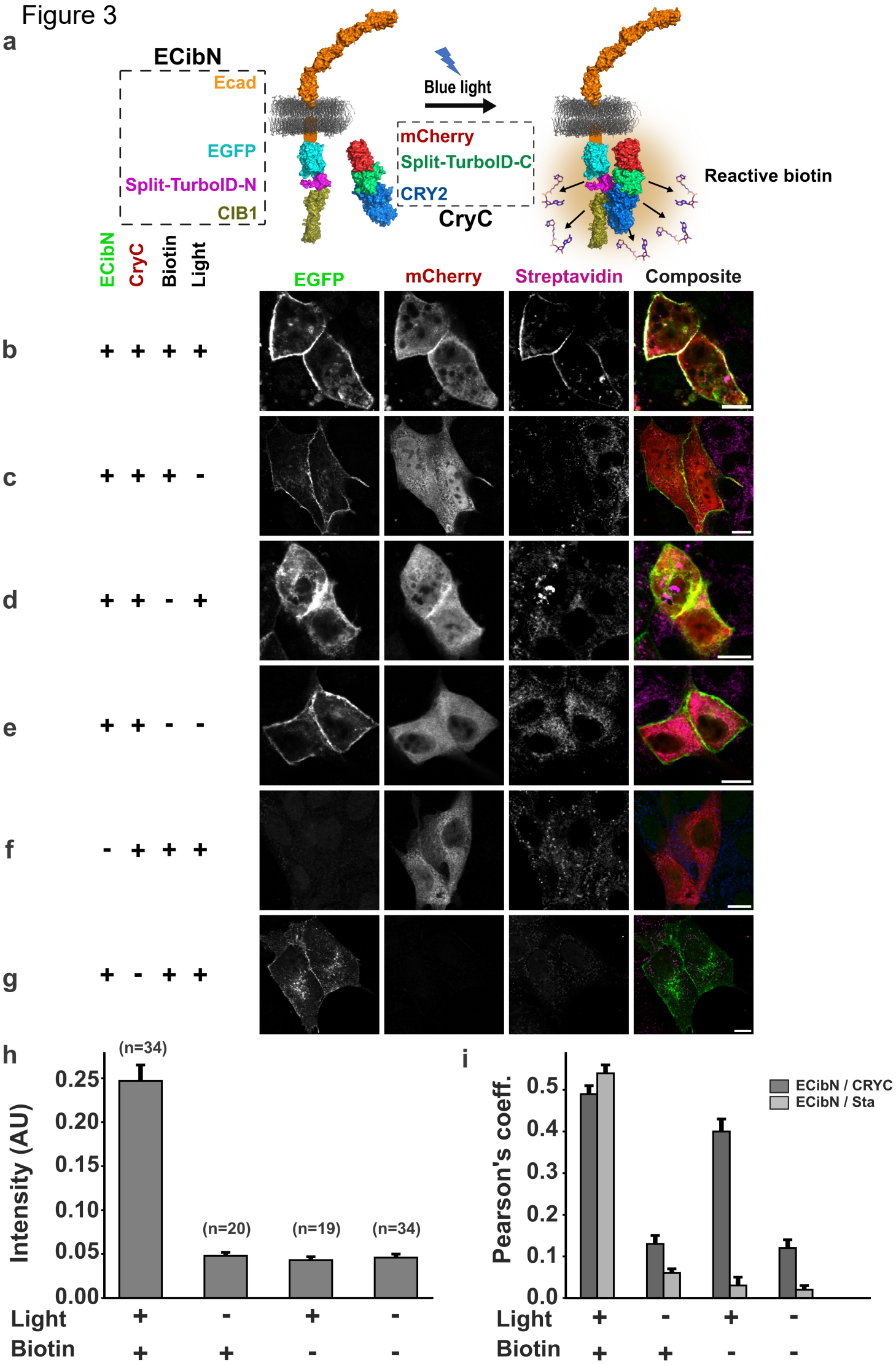
a
ECibN
Ecad
EGFP
Split-TurboID-N
CIB1
Blue light
mCherry
Split-TurboID-C
CRY2
CryC
Reactive biotin
ECibN
CryC
Biotin
Light
EGFP
mCherry
Streptavidin
Composite
b + + + +
c + + + -
d + + - +
e + + - -
f - + + +
g + - + +
h
Intensity (AU)
0.25
0.20
0.15
0.10
0.05
0.00
(n=34)
(n=20)
(n=19)
(n=34)
Light + - + -
Biotin + + - -
i
Pearson's coeff.
0.5
0.4
0.3
0.2
0.1
0.0
ECibN / CRYC
ECibN / Sta
Light + - + -
Biotin + + - -

Figure 4

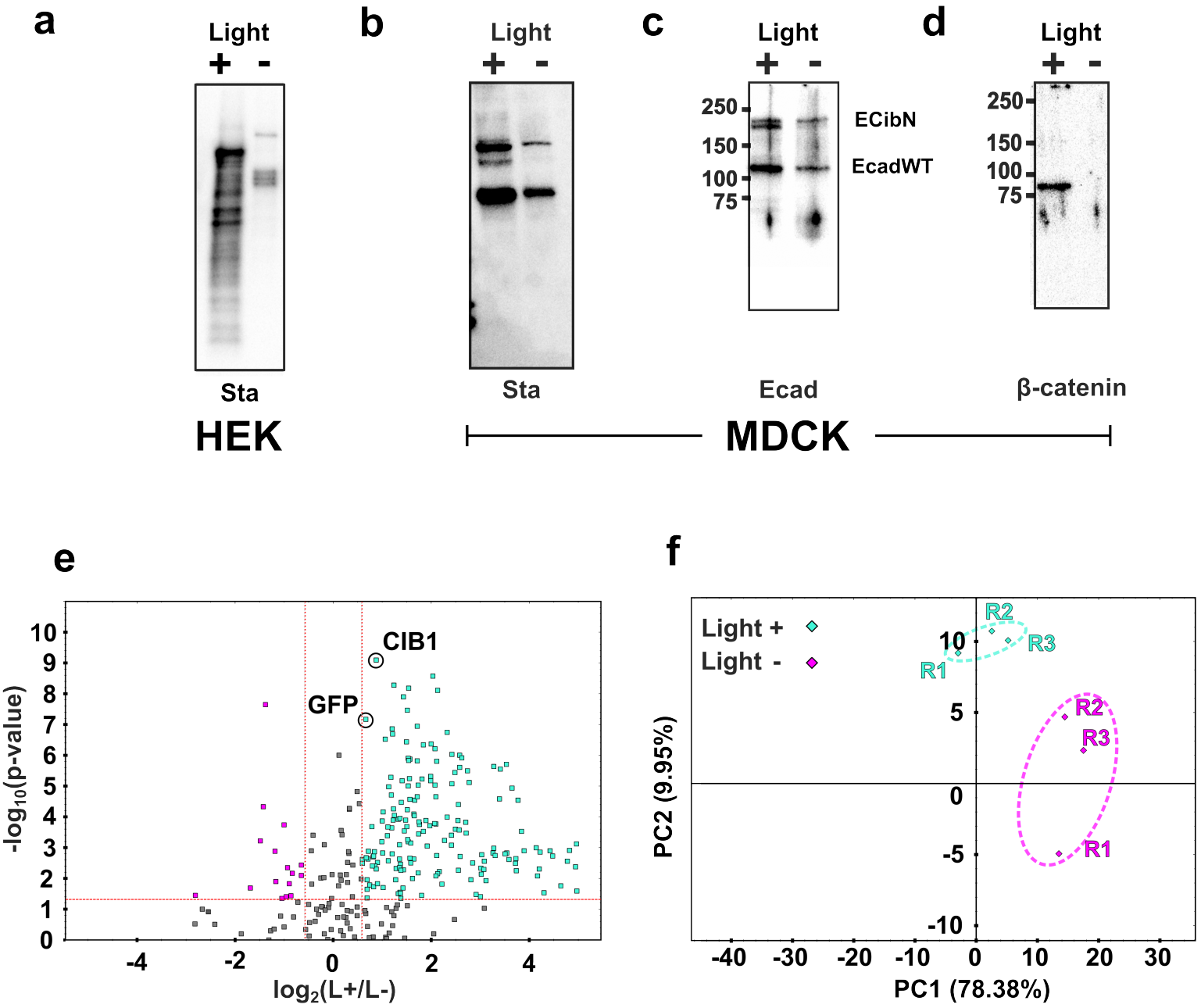
a
Light
+ -
Sta
HEK
b
Light
+ -
Sta
c
Light
+ -
250
150
100
75
ECibN
EcadWT
Ecad
d
Light
+ -
250
150
100
75
β-catenin
MDCK
e
CIB1
GFP
-log10(p-value)
log2(L+/L-)
f
Light +
Light -
R1
R2
R3
PC2 (9.95%)
PC1 (78.38%)